Dysregulation of SREBP2 induces BACE1 expression.

DYSREGULATION OF SREBP2 INDUCES BACE1 EXPRESSION

Abbreviated title: SREBP2 induces BACE1

Raffaella Mastrocola[1], PhD, Michela Guglielmotto[1,2], PhD, Claudio Medana[3], PhD, Maria Graziella Catalano[4], MD, Santina Cutrupi[5], PhD, Roberta Borghi[6], PhD, Elena Tamagno[1,2], PhD, Giuseppe Boccuzzi[4], MD, Manuela Aragno[1], PhD.

Affiliations: [1]Department of Experimental Medicine and Oncology, University of Turin, Italy; [2]Neuroscience Institute of the Cavalieri Ottolenghi Foundation (NICO); [3]Department of Analytical Chemistry, University of Turin, Italy; [4]Department of Clinical Pathophysiology, University of Turin, Italy; [5]Department of Animal and Human Biology, University of Turin, Italy; [6]Department of Neuroscience, Ophtalmology and Genetics, University of Genoa, Italy.

Corresponding author:

Raffaella Mastrocola, PhD - Dept. of Experimental Medicine and Oncology - General Pathology section - University of Turin - C.so Raffaello 30 - 10125 Torino, Italy - Tel: +390116707758 - Fax: +390116707753 - E-mail address: raffaella.mastrocola@unito.it

Key words: SREBP2; BACE1; Alzheimer's disease; cholesterol synthesis; high-fat diet

Abstract

β-amyloid hyperproduction has been observed in response to alterations in neuronal intracellular cholesterol storage, efflux, and synthesis, induced in rats by a high-fat diet. It has been suggested that cholesterol homeostasis is altered in Alzheimer's disease resulting in higher β- and γ-secretase activity. In the current study the neuronal activation status of sterol regulatory element binding protein 2 (SREBP2) as well as its involvement in β-secretase BACE1 activity was investigated in high-fat fed rats (26% fat and 4% cholesterol for 20 weeks), and in SK-N-BE neuroblastoma cells exposed to 20 μM cholesterol. This work demonstrates that in brain a hyperlipidic diet is able to induce a hyper-expression of BACE1 and to determine an unbalance in cerebral cholesterol homeostasis so that SREBP2 is activated. In addition, we show for the first time the involvement of SREBP2 on expression of BACE1 in SK-N-BE cells exposed to high cholesterol. Although the enhanced risk of Alzheimer's disease in metabolic syndrome is related to several factors, our results suggest that SREBP2, which can be modulated by the impairment of cerebral cholesterol homeostasis, has a direct role on BACE1 expression and may be involved in Alzheimer's disease progression.

Introduction

Recent studies indicate that alterations in cholesterol metabolism induced by a high-fat diet influence some molecular mechanisms involved in neurodegenerative diseases, such as Niemann-Pick, Huntington's disease, prion diseases, and Alzheimer's disease (AD) (Bach et al., 2009; Bi and Liao, 2010; Block et al., 2010; Lütjohann et al., 2000; Solomon, et al., 2009), even if controversial data have been reported (Hoyer and Riederer, 2007; Ishii et al., 2003; Zandi et al., 2005). Our study investigates a new potential link between diet-induced alterations in brain cholesterol metabolism and the β-site APP-cleaving enzyme 1 (BACE1) overexpression which represents an early event in AD development.

The CNS contains as much as 23% of total body cholesterol (Dietschy and Turley, 2004) and, since the blood brain barrier (BBB) is nearly impermeable to plasma lipoprotein-associated cholesterol, almost all of brain cholesterol is locally synthesized (Bjorkhem and Meaney, 2004). Excess of cholesterol is exported from brain in the form of oxysterols which can cross the BBB. The major oxysterol in the brain is the 24S-hydroxycholesterol (24-OH-chol) which regulates genes involved in intracellular free-cholesterol modulation (Wang et al., 2007).

Brain cholesterol synthesis is tightly regulated by a feedback system based on the activity of sterol regulatory element-binding proteins 2 (SREBP2). In its inactivated form, SREBP2 is retained in the endoplasmic reticulum (ER) by two inhibitory proteins, SCAP and Insig. When cholesterol *de novo* synthesis is required, SREBP2 is cleaved and translocated to the nucleus, where it activates target genes involved in cholesterol synthesis and uptake (Bengoechea-Alonso and Ericsson, 2007; Goldstein et al., 2006). In contrast, when the intracellular levels of cholesterol increase, SREBP2 is down-regulated. Thus, a proper SREBP2 intracellular traffic is crucial for its activity. Indeed, it has been recently reported an up-regulation of SREBP2 in prion-infected neuroblastoma cells. In this study

authors suggest that changes in intracellular cholesterol distribution by prion-infection lead to its local decrease at the level of ER and this cause an activation of SREBP2 and cholesterol biosynthesis (Bach et al., 2009). SREBP2 controls the expression of enzymes involved in cholesterol synthesis. One of the target genes activated by SREBP2 is that encoding for the enzyme hydroxy-methylglutaryl-Coenzyme A reductase (HMG-CoA-R), the rate limiting enzyme in the process of cholesterol synthesis (Bengoechea-Alonso and Ericsson, 2007).

Intracellular cholesterol dynamics can be influenced by several factors and a high fat diet is among these. High cholesterol diet leads to metabolic disturbances including obesity, insulin resistance and dislipidemia and may contribute, at least in part, to the development of brain diseases through the action of key mediators such as trophic factors support alterations, mitochondrial abnormalities, oxidative stress increase, and intracellular cholesterol homeostasis failure (Zhang et al., 2009; Koudinov and Koudinova, 2005). Moreover, several studies report that alterations in both plasma and in brain cholesterol levels are related to AD disease (Kivipelto et al., 2006; Puglielli et al., 2003; Simons et al., 2001; Solomon, et al., 2009). Others studies, demonstrating a possible beneficial effect of cholesterol lowering drugs, such as statins or 7-dehydrocholesterol reductase inhibitors, against AD development, support this hypothesis (Kirsch et al., 2003; Tong et al., 2009; Parsons et al., 2007). Indeed, in hypercholesterolemic patients, statins reduce serum β-amyloid peptides (Aβ) levels (Buxbaum et al., 2002; Friedhoff et al., 2001), even if others data are conflicting (Ishii et al., 2003; Serrano-Pozo et al., 2010). However, a recent therapeutic approach to ameliorate amyloid pathology has proposed to act on cholesterol synthesis or on inhibition of the activity of specific enzymes correlated to conversion between free cholesterol and cholesterol esters (Bryleva et al., 2010; Parsons et al., 2007).

The abnormal generation and deposition of Aβ are the pathologic hallmark of AD. Aβ is generated by two sequential proteolytic cleavage steps from the β-amyloid precursor protein (βAPP) (Haas, 2004) that is initially cleaved by the β-secretase BACE1, which has been identified as a β-site APP-cleaving transmembrane aspartic protease. This cleavage is followed by the subsequent proteolysis of the membrane-bound C-terminal fragment catalyzed by the γ-secretase complex (Vassar, 2001). Hypercholesterolemia is linked to increased Aβ production and deposition in the brain both in humans (Pappolla et al., 2003; Kivipelto and Solomon, 2006) and in animals (Thirumangalakudi et al., 2008; Ghribi et al., 2006) and is linked to an increased risk of developing AD (Rushworth and Hooper, 2011). Moreover, Aβ hyperproduction has been observed in response to alterations in neuronal intracellular cholesterol storage, efflux, trafficking, and synthesis, induced in rats by a high-fat diet (Koudinov and Koudinova, 2005) and it has been suggested that cholesterol homeostasis is altered in AD brains resulting in higher β- and γ-secretase activity (Xiong et al., 2008).

In the current study the neuronal activation status of SREBP2 as well as its involvement in BACE1 activity were investigated in *in vivo* experimental conditions mimicking a cholesterol-rich Western diet feeding and in high cholesterol-exposed SK-N-BE neuroblastoma cells.

Materials and Methods

All compounds were purchased from Sigma Chemical Co. (St. Louis, MO, USA) and materials for real-time PCR were from Bio-Rad Laboratories (Hercules, CA, USA), unless otherwise stated.

Animals and treatments

Male Wistar rats (Harlan Laboratories, Udine, Italy) weighing 200–220 g were cared for in compliance with the Italian Ministry of Health Guidelines (No. 86/609/EEC) and with

the Principles of Laboratory Animal Care (NIH No. 85–23, revised 1985). The scientific project, including animal care, was supervised and approved by the local ethical committee. The animals were divided into two groups: CTRL-group, fed a standard lab chow, consisting of 24% proteins, 5% fats, and 50.3% carbohydrates (p/w); and HF-group, fed a high-cholesterol diet, consisting of 17% proteins, 10.1% fats, 4% cholesterol and 51.6% carbohydrates. Both diets contained a standard mineral and vitamin mixture (Deng et al., 2007). Both groups received water *ad libitum*. Body weight and food intake were recorded weekly. After 20 weeks of respective diets, rats were anesthetized with 20 mg/kg bw of Zoletil 100 (Virbac S.r.l., Carros, France) and killed by aortic exsanguination. Blood was collected and plasma isolated. The brain was rapidly isolated, hemispheres were separated, snap-frozen in N2 and stored at −80°C.

Oral glucose tolerance test

Before killing, after a fasting period of 12 h, basal glycemia was measured via saphenous vein puncture using a glucometer (Accuchek; Roche Diagnostics, Mannheim, Germany). Then, a 50% (w/v) glucose solution was administered orally at 3 g/kg. Plasma glucose levels were measured at several time points after glucose loading.

Biochemical parameters

Plasma lipid profile was determined by measuring the contents of triglycerides (TG), total cholesterol (TC), cholesterol associated to high-density lipoproteins (HDL), and to low-density lipoproteins (LDL) by standard enzymatic procedures using reagent kits (Hospitex Diagnostics, Florence, Italy).

Plasma insulin level was measured using an enzyme-linked immunosorbent assay (ELISA) kit (Mercodia AB, Uppsala, Sweden).

Insulin sensitivity was calculated using the homeostasis model assessment (HOMA): fasting glucose (mmol/l)×fasting insulin (μg/l)/22.5.

Cell culture

SK-N-BE neuroblastoma cells were maintained in RPMI (Roswell Park Memorial Institute) 1640 medium containing 2 mM glutamine and supplemented with 10% fetal bovine serum, 1% non-essential amino acids, 1 mM sodium pyruvate, and a 1% antibiotic mixture (penicillin–streptomycin–amphotericin), in a humidified incubator at 37°C with 5% CO2. For differentiation, 2 x 10^6 cells were plated in 75 cm^2 culture flasks (Costar, Lowell, MA, USA) and treated with10 µM retinoic acid for 10 days. Cholesterol diluted in ethanol was added to 20 µM for up to 48 hours of incubation.

Preparation of tissue extracts

For cytosolic and nuclear proteins extraction rat brains were homogenized at 10% (w/v) using a Potter Elvehjem homogenizer (Wheaton, NJ, USA) in a homogenization buffer containing 20 mM HEPES, pH 7.9, 1 mM $MgCl_2$, 0.5 mM EDTA, 1 mM EGTA, 1 mM dithiothreitol (DTT), 0.5 mM phenylmethylsulphonyl fluoride (PMSF), 5 µg/ml aprotinin, and 2.5 µg/ml leupeptin. Homogenates were cleared by centrifugation at 1,000 g for 5 min at 4°C. Supernatants were removed and centrifuged at 15,000 g at 4°C for 40 min to obtain the cytosolic fraction. The pelleted nuclei were resuspended in an extraction buffer containing 20 mM HEPES, pH 7.9, 1.5 mM $MgCl_2$, 0.2 mM EDTA, 20% (w/v) glycerol, 1 mM EGTA, 1 mM DTT, 0.5 mM PMSF, 5 µg/ml aprotinin, and 2.5 µg/ml leupeptin. The suspensions were incubated on ice for 30 min for high-salt extraction followed by centrifugation at 15,000 g for 20 min at 4°C. The resulting supernatants containing nuclear proteins were carefully removed and stored.

Total extracts were obtained from a 10% (w/v) rat brain homogenate in RIPA buffer containing 0.5% Nonidet P-40, 0.5% sodium deoxycholate, 0.1% SDS, 10 mmol/l EDTA, and protease inhibitors. After 40 minutes of incubation in ice homogenates were cleared by centrifugation at 15,000 g at 4°C for 40 min. Supernatants were removed and stored.

Preparation of cell lysates and nuclear extracts from culture cells was performed as previously described (Tamagno et al., 2005).

Protein content was determined using the Bradford assay. Protein extracts were stored at −80°C until use.

Cholesterol and 24-OH-cholesterol analysis with LC-MS

Free cholesterol and 24-OH-cholesterol were evaluated on plasma and on cytosolic extracts from rat brains and SK-N-BE cells. Samples aliquots of 0.2 ml were thawed and spiked to 130 ng/ml with 24-hydroxy cholesterol-25, 26, 27 $^{13}C_3$ in methanol. Saponification was performed at 37 °C for 1 h after the addition of 1 mL of freshly prepared 0.9 M sodium hydroxide in 9:1 ethanol:water. Saturated aqueous sodium chloride (0.5 ml) was added, and the aqueous phase was extracted twice with 2.0 ml of hexane. The dried organic extract residue was reconstituted in 200 µl of HPLC mobile phase

The chromatographic separations were run on a Phenomenex Luna C18 column, 150 × 2.0 mm, 3 µm particle size (Phenomenex, Castel San Pietro Terme, BO, Italy). Injection volume was 20 µl and flow rate 0.2 ml/min. Gradient mobile phase composition was adopted: 60:40 to 100:0 methanol:aqueous ammonium acetate 0.1 mM in 15 min. A LCQ Orbitrap ion trap mass spectrometer (Thermo Scientific, Bremen, D) equipped with an atmospheric pressure interface and an APCI ion source was used. The LC column effluent was delivered into the ion source using nitrogen as sheath and auxiliary gas. The APCI vaporizer temperature was set at 320°C and the corona discharge voltage at the 6.0 kV value. The heated capillary value was maintained at 275°C. The acquisition method used was previously optimized in the tuning sections for the analyte ion (capillary, magnetic lenses and collimating octapoles voltages) in order to achieve the maximum of sensitivity. Spectra were acquired in the positive FTMS (50-900 *m/z* range) and FTMS/MS mode (precursor ions 369, 385 and 372, 100-395 *m/z* range, normalized collision energy 30%).

Western blotting

Total or nuclear proteins were separated by SDS-PAGE and electrotransferred to nitrocellulose membrane. After blocking in 5% nonfat milk, membranes were incubated with a rabbit anti-HMG-CoA-R antibody (Upstate, Lake Placid, NY, USA), a rabbit anti-BACE1 antibody (Chemicon, Temecula, CA, USA), and a mouse anti-SREBP2 antibody (Santa Cruz Biotechnology, Santa Cruz, CA, USA) overnight at 4°C. After washing, appropriate secondary horseradish peroxidase–linked (Amersham-Pharmacia Biotech Italia, Cologno Monzese, Italy) antibodies were added.

Detection was performed using ECL chemiluminescence substrate (Amersham). Specific bands were quantified by densitometry using analytic software (Bio-Rad, Quantity-One, Munchen, Germany). β-actin served as loading control for total protein extracts, and lamin A for nuclear extracts.

Real time RT-PCR

Total RNA was isolated using the TriPure isolation reagent (Roche Diagnostics, Monza, Italy). One microgram of total RNA was reverse-transcribed using the iScript cDNA synthesis kit (Roche).

Primers were designed using the Beacon Designer 5.0 program and applying the parameters outlined in the Bio-Rad iCycler manual.

Specificity of the primers was confirmed by BLAST analysis. The following primers were used:

Rat BACE-1:

5′-GCATGATCATTGGTGGTATC-3′ - 5′-CCATCTTGAGATCTTGACCA-3′.

Rat SREBP2:

5′-CACTCACGCTCCTCGGTCAC-3′ - 5′-CGGATAAGCAGGTCTGTAGGTTGG-3′.

Rat β-actin:

5’-CCA CAC CCGCCACCAGTTC-3’ - 5’-GACCCATACCCACCATCACACC-3’

Rat β2-microglobulin:

5’-TCTTTCTGGTGCTTGTCTCTCTGG-3’- 5’-CTATCTGAGGTGGGTGGAACTGAG-3’

Rat L13A:

5’-AGGTGGTGGTTGTACGCTGTG-3’ - 5’-GGTTGGTGTTCATCCGCTTTCG-3’

Human BACE-1:

5′-CATTGGAGGTATCGACCACTCGCT-3′- 5′-CCACAGTCTTCCATGTCCAAGGTG-3′.

Human SREBP2:

5’-AGCAGATGGGCAGCAGAGTTC-3’ - 5’-TGAGGGCAGGGTCAGAGGTG-3’

Human β-actin:

5′-GGCACTCTTCCAGCCTTCCTTC-3′- 5′-GCGGATGTCCACGTCACACTTCA-3′.

Human β2-microglobulin:

5’-AGA TGA GTA TGC CTG CCG TGT G-3’ - 5’-TCA ACC CTC CAT GAT GCT GCT TAC-3’

Human L13A:

5’-GCA AGC GGA TGA ACA CCA ACC-3’ - 5’-TTG AGG GCA GCA GGA ACC AC-3’

Real-time PCR was performed using a Bio-Rad iQ iCycler detection system with SYBR green fluorophore. Reactions were run in a total volume of 25 μl, including 12.5 μl of IQ SYBR Green Supermix, 0.5 μl of each primer at 10 μM concentration, and 5 μl of the previously reverse transcribed cDNA template. The protocol used was denaturation (95 °C for 5 min) and then amplification repeated 40 times (95 °C for 15 s, 60 °C for 1 min). A melting curve analysis was made after each run to ensure a single amplified product for every reaction. All reactions were run at least in triplicate for each sample. Gene expression was normalized against β-actin, L13A, and β2-microglobulin as house-keeping genes.

Chromatin immunoprecipitation assay (ChIP)

Chromatin was prepared from 10-cm-diameter plate per sample. Cross-linking was performed with 1% formaldehyde for 10 min at room temperature. The reaction was quenched by 125 mM glycine for 10 min at room temperature. After 2 washes with ice-cold PBS, cells were scraped in 1 ml PBS, 0.5 mM PMSF, and protease inhibitor mixture

(Roche) and collected by centrifugation. The cell pellet was lysed in 400 µl of 1% SDS, 10 mM EDTA, 50 mM Tris pH 8, 0.5 mM PMSF, and protease inhibitor mixture (Roche) and sonicated at 4°C for 10 cycles 30-sec rounds followed by a 60-sec pause, at an amplitude of Misonix XL2020. DNA shearing efficiency was evaluated by fractionating the DNA extracted from sheared, de-cross-linked chromatin on an agarose gel to ensure a DNA fragment size enriched between 300 and 1,000 bp. The lysate was clarified by centrifugation, and sheared chromatin was diluted in 0.01% SDS, 1.1% Triton X-100, 1.2 mM EDTA, 16.7 mM Tris pH 8, 167 mM NaCl, 0.5 mM PMSF, and protease inhibitor mixture (Roche). An aliquot of 100 µl of diluted chromatin extract was retained as total input control. Immunoprecipitations were performed by incubating 1 ml of sheared chromatin with 2 µl of anti-SREBP2 serum (Santa Cruz) overnight at 4°C. Upon the addition of protein A Sepharose (GE Healthcare), samples were incubated on a rotating platform at 4°C overnight and then centrifuged for 2 min at 3,000 *g*. Beads were washed once with each of the following buffers: wash buffer 1 (0.1% SDS, 1% Triton X-100, 2 mM EDTA, 20 mM Tris pH 8, 150 mM NaCl), wash buffer 2 (0.1% SDS, 1% Triton X-100, 2 mM EDTA, 20 mM Tris pH 8, 500 mM NaCl), wash buffer 3 (1 mM EDTA, 10 mM Tris pH 8, 1% Nonidet P-40, 1% sodium deoxycholate, 0.25 M LiCl) and wash buffer 4 (10 mM Tris pH 8, 1 mM EDTA). The beads and the diluted chromatin for the total input DNA were subsequently incubated with 100 µl of 10% Chelex (Bio-Rad) at 95°C for 10 min to reverse the cross-link and then incubated with Proteinase K (Invitrogen) for 30 min at 55°C. Proteinase K was inactivated for 10 min at 95°C followed by full-speed centrifugation for 2 min. Supernatants were diluted and used for PCRs. Primers for PCR amplification were designed by using the program Primer3 to obtain an amplicon size of 150 bp. Specific sequences from immunoprecipitated and input DNA were detected by quantitative real-time

PCR and SYBR Green-detection (Stratagene) BACE 1 promoter (forward, 5'-CCT GCC ATG GGA AGA CTA CA-3' and reverse, 5'- CTG CTC AGG CCA CCA TAA TC -3').

RNA interference

To knockdown SREBP2 expression in differentiated neuroblastoma cells we used siRNA duplex (Qiagen, Milano, Italy). The following targeting sequence was used: 5'-CCGCAGTGTCCTGTCATTCGA-3'.

The siRNA and related non/silencing control (negative control) were transfected in neuroblastoma cells with Lipofectamine transfection reagent (InVitrogen, Milano, Italy) according to the manufacturer's instructions for 48 hours. In order to improve the silencing technique, we re-trasfected cells with siRNA or non silencing control at the intermediate point of 36 hour.

Statistical analysis

All values are expressed as means ± SD and were analyzed by student's *t*-test followed by Bonferroni's post-test. A p value <0.05 was considered statistically significant.

Results

High fat diet in rats induces alterations in body weight, glucose tolerance, plasma lipid profile and brain cholesterol metabolism.

As shown in **Figure 1, panel A**, rats fed a high-fat diet (HF rats) for 20 weeks showed a significant increase in body weight compared to control rats (CTRL) (+30%), paralleled at insulin resistance onset (insulin plasma levels +270%, HOMA index +150%). Fasting blood glucose concentration was unchanged in both experimental groups.

Before the sacrifice of the animals, an oral glucose tolerance test (OGTT) was performed. As reported in **Figure 1, panel B**, the glycemic curve in HF rats significantly moved away compared to CTRL curve 90 minutes after oral glucose charge, indicating a reduced glucose tolerance induced by the high-fat diet.

After 20 weeks of dietetic regimen, HF-rats showed a marked alteration on plasma lipid profile (**Table 1**) featured by increased levels of triglycerides (+150%), of total cholesterol (+63%), and of LDL-cholesterol (+340%), beside a decreased level of HDL-cholesterol (-60%). A marked increase (+100%) in 24-OH-chol plasma levels in HF rats compared to CTRL (**Table 2**) was found.

In brains, the level of total cholesterol was unchanged between CRTL and HF groups (35.2 ± 4.9 vs 44.9 ± 8.7 μmoles/g tissue) while the level of free cholesterol was higher in CRTL group with respect to HF group (38.15 ± 8.83 ng/mg prot vs 22.55 ± 4.76 ng/mg prot). Moreover, the levels of 24-OH cholesterol in the brain were significantly increased (+50%) in HF rats compared to CTRL (**Table 2)**.

High fat diet induces SREBP2, cholesterol synthesis and BACE1 expression in rat brain.

As shown in **Figure 2, panel A**, HF rats showed a significant increase in SREBP2 mRNA expression as well as in BACE1 mRNA expression when compared to control animals.

SREBP2 and BACE1 protein levels paralleled results obtained by real-time PCR. HF diet induced a strong increase of active form of SREBP2 both in total brain extract (lower band) and in nuclear fraction (+120% and +100%, respectively) (**Figure 2, panels B and C**)**.** As shown in Figure 2 panel B, a band corresponding to the inactive SREBP2 isoform (upper band), that also appear markedly increased in HF rats, was evident in total extracts .

To confirm the enhanced cholesterol synthesis in HF-rats brain, HMG-CoA-reductase was detected. **Figure 2, panels D and F,** shows an increase of HMG-CoA-R protein levels in HF brains vs CTRL (+100%).

Similarly, BACE1 protein levels were significantly increased (about +50%) in HF rats compared to controls, as reported in **Figure 2, panels E and F.**

Cholesterol addition in differentiated SK-N-BE neuroblastoma cells induces SREBP2 and BACE1 overexpression

To better understand the relationship between overexpression of SREBP2 and hyper-regulation of BACE1, differentiated SK-N-BE cells were exposed to 20 μM cholesterol for up to 48 hours. Cells treated with cholesterol showed a significant decrease in intracellular free cholesterol level during the time of exposition, evaluated with mass spectrometry technique, that appeared significantly decreased after 12 hours and halved its level between 16 and 24 hours of incubation (**Figure 3, panel A).** Levels of 24-OH cholesterol presented an opposite course, thus its levels significantly increased (+100%) between 12 and 24 hours of incubation (**Figure 3, panel B**).

Cells treated with cholesterol showed a significant increase in SREBP2 (2 fold) and BACE1 (2.5 fold) mRNA expression after 12 hours of incubation (**Figure 4, panel A**). To better characterize the relationship between SREBP2 and BACE1 we performed a ChIP assay, to determine whether SREBP2 protein was associated with specific genomic region of BACE1on promoters or other DNA binding site. In order to verify if BACE1 is a putative target of SREBP2 we analyzed BACE promoter using Transfac program and we identified SREBP-binding motif spanning from –1192 to –1181bp. Therefore, we investigated whether the proximal portion of endogenous BACE promoter may bind SREBP2 during cholesterol treatment. ChIP analysis of SREBP-2 was performed in differentiated SK-N-BE cells and showed that SREBP2 is bound to the region containing consensus site (**Figure 4, panel B**).

The protein levels of the nuclear SREBP2 activated form were also induced by treatment with cholesterol. As shown, only after 12 hours of cholesterol treatment a significant increase (2 fold) in activated form of SREBP2 was evident (**Figure 5, panels A and B**). Accordingly, the protein levels of HMG-CoA-reductase, were significantly increased after 16 hrs of incubation of cholesterol (**Figure 5, panel C and D**).

Treatment with cholesterol was also followed by a strong increase of BACE1 protein levels that peaked after 20 hours of incubation and persisted for up to 48 hours (**Figure 5, panels E and F**).

Finally, the involvement of SREBP2 in BACE1 up-regulation was directly confirmed by silencing SREBP2 using RNA interference (**Figure 6**). Blocking SREBP2 expression, as expected, almost completely blocked up-regulation of BACE1 by cholesterol treatment (**Figure 6, panels A and B**).

Discussion

High cholesterol levels may be detrimental to human neurological functions, although either positive, negative and null correlations between cholesterol levels and impaired cognitive functions have been reported by several studies (Hoyer and Riederer, 2007; Ishii et al., 2003; Kivipelto and Solomon, 2006; Pappolla et al., 2003; Zandi et al., 2005).

In the current study we demonstrate an up-regulation of SREBP2 and BACE1 in the brain of rats fed a high cholesterol diet as well as in SK-N-BE neuroblastoma cells exposed to high cholesterol levels. We reported alterations in crucial cerebral molecular pathways, such as cerebral cholesterol homeostasis and synthesis, evoked by increased peripheral cholesterol levels.

Although it is not clear how plasma cholesterol affects brain functions, it has been proposed that enhanced blood cholesterol may be metabolized to its oxysterols, oxygenated derivates that can cross lipophilic membranes (Björkhem, 2002), and, thus, enter the brain. In fact, increased brain levels of 27-hydroxycholesterol have been measured in AD patients (Björkhem et al., 2006).

Moreover, in neurons the exceeding intracellular cholesterol is converted in 24-OH-chol to be exported from neurons to the blood, or it is stored either in cell membranes or, as

cholesterol ester, in cytoplasmic lipid droplets. Since almost all of the plasma 24-OH-chol is generated in the brain (Bjorkhem and Meaney, 2004), our observation that 24-OH-chol levels are increased in both cerebral tissue and plasma of HF-fed animals suggests that the cerebral cholesterol turnover is enhanced in the presence of a high cholesterol intake. The increase in the conversion rate of free cholesterol to 24-OH-chol was convincingly confirmed by *in vitro* experiments on SK-N-BE cells exposed to high cholesterol concentrations. Interestingly, our data are in keeping with clinical studies showing that the 24-OH-chol concentrations are increased in plasma and in cerebrospinal fluid of patients in early phases of AD, probably as a result of the enhanced turnover of cholesterol in neurons (Lütjohann et al., 2000).

High extracellular levels of cholesterol have been previously demonstrated to induce an unbalance in intracellular cholesterol esterification and compartimentalization (Björkhem, 2002), which exerts an important role in Aβ deposition, and recent studies suggest that unbalanced cholesterol homeostasis can be affected by SREBP2 activity (Puglielli et al., 2003). In addition, it has been reported that inhibition of ACAT1, the major functional enzyme in brain that convert free cholesterol to cholesterol esters, increases in mice the conversion rate of cholesterol to 24-OH-chol, and increases in hippocampal neuronal cells cholesterol and 24-OH-chol levels in ER, decreasing in both models the cholesterol synthesis and leading to a reduction in APP levels (Bryleva et al., 2010; Prasanthi et al., 2009).

Here we suggest that the reduction of free cholesterol observed in brain of rats fed a high fat diet, as well as in SK-N-BE cells exposed to cholesterol after 12 hrs, leads to SREBP2 activation.

Most notably, we demonstrate for the first time that SREBP2 activation evoked by high cholesterol exposure is associated with BACE1 hyperexpression, both *in vivo* and *in*

vitro experimental models. It is reported that M19 cells, in which SREBP2 never becomes active, have significantly decreased free cholesterol and unaltered Aβ levels. In contrast, 25RA cells, in which SREBP2 is constitutively active, have normal free cholesterol and increased cholesterol ester levels and elevated Aβ levels (Puglielli et al., 2001). Thus, it is conceivable a correlation between SREBP2 and BACE1 activation.

Moreover, we observed by chromatin immunoprecipitation analysis that the promoter of BACE1 contains a consensus site for SREBP2, and that the activated form of SREBP2 effectively binds to the BACE1 promoter in response to cholesterol treatment. Cloning and detailed analysis of the promoter region of BACE and of the 5′ untranslated region of the BACE mRNA (5′ UTR) have been reported (Sambamurti et al., 2004). These regions contain multiple transcription factor binding sites, such as AP1, AP2, CREB, ERE, GRE, NF-κB, STAT1, SP1 (Bourne et al., 2007; Sambamurti et al., 2004). The identification of transcription factors and of intracellular signaling involved in the activation of BACE1 in brain may provide new targets to specifically interfere with BACE1 expression and to Aβ generation.

In addition, the direct causal role of SREBP2 on BACE1 expression was here confirmed by SREBP2 silencing. The cholesterol-induced overexpression of BACE1 in SK-N-BE cells was no more detectable after the silencing of SREBP2.

Since it is known that the activity of Aβ-synthesizing enzymes, the β- and γ-secretases that are located in cholesterol-rich lipid rafts, may be positively modulated by high cholesterol concentrations (Cordy et al., 2003; Wolozin, 2004), our observation that BACE1 expression is directly regulated by SREBP2 transcriptional activity adds new insights on the complex molecular mechanism underlying cholesterol-induced brain damage. Inhibition of cholesterol synthetizing enzymes by statins or other inhibitors leads to a reduction of Aβ generation through the inhibition of BACE1 dimerization and alteration

of its sub-cellular localization (Parsons and Austen, 2005; Parsons, et al 2007). Here we demonstrate that inhibition of SREBP2 prevents the BACE1 activity acting at the transcriptional level.

We are aware that *in vivo* factors other than hypercholesterolemia may be involved in the enhanced BACE1 expression in HF-rats, such as hyperinsulinemia or prolonged postprandial hyperglycemia, as suggested by other authors (Ho et al., 2004; Guglielmotto et al., 2010). In fact, it has been observed that NIDDM-like insulin resistance in mice might influence signal transduction mechanisms, such as activation of GSK-3, which are known to promote amyloidogenic Aβ peptides generation (Ho et al., 2004). We have also previously demonstrated that hyperglycemia, through AGEs, leads to increased BACE1 expression (Guglielmotto et al., 2010). In addition, another risk factor for Aβ generation could be represented by the reduced level of serum HDL cholesterol rather than by the increased level of serum total or LDL cholesterol (Michikawa, 2003).

However, previous findings show that cholesterol affect the APP processing by enhancing BACE1 activity (Raffai and Weisgraber, 2003; Simons et al., 2001; Shobab et al., 2005). Indeed, various animal studies have shown that hypercholesterolemia leads to dysfunction of the cholinergic system, cognitive deficits, beta-amyloid and tau-pathology, all characteristics of AD, and that a high-cholesterol diet can induce some AD-like pathologies in *in vivo* models (Granholm et al., 2008; Refolo et al., 2000; Ullrich et al., 2010).

Our results suggest that the dysregulated activation of SREBP2 induced by an impairment of cerebral cholesterol homeostasis has a role on BACE1 expression. Thus, our study proposes a new potential molecular pathway linking a high-cholesterol diet and BACE1 up-regulation.

Acknowledgments

This study was supported by the Regione Piemonte “Progetto di Ricerca Sanitaria Finalizzata 2009”, by the CRT Foundation 2009: “Il diabete come fattore di rischio per l’insorgenza della malattia di Alzheimer”, Turin, Italy, and by the PRIN 2007.

References

Bach C, Gilch S, Rost R, Greenwood AD, Horsch M, Hajj GN, Brodesser S, Facius A, Schädler S, Sandhoff K, Beckers J, Leib-Mösch C, Schätzl HM, Vorberg I. Prion-induced activation of cholesterogenic gene expression by SREBP2 in neuronal cells. J Biol Chem 2009;284:31260-9.

Bengoechea-Alonso MT, Ericsson J. SREBP in signal transduction: cholesterol metabolism and beyond. Curr Opin Cell Biol 2007;19:215-22.

Bi X, Liao G. Cholesterol in Niemann-Pick Type C disease. Subcell Biochem 2010;51:319-35.

Björkhem I, Heverin M, Leoni V, Meaney S, Diczfalusy U. Oxysterols and Alzheimer's disease. Acta Neurol Scand Suppl 2006;185:43-9.

Bjorkhem I, Meaney S. Brain cholesterol: long secret life behind a barrier. Aterioscler Tromb Vasc Biol 2004;24:806-15.

Björkhem I. Do oxysterols control cholesterol homeostasis? J Clin Invest 2002;110(6):725-30.

Block RC, Dorsey ER, Beck CA, Brenna JT, Shoulson I. Altered cholesterol and fatty acid metabolism in Huntington disease. J Clin Lipidol 2010;4:17-23.

Bourne KZ, Ferrari DC, Lange-Dohna C, Rossner S, Wood TG, Perez-Polo JR. Differential regulation of BACE1 promoter activity by nuclear factor-kappaB in neurons and glia upon exposure to beta-amyloid peptides. J Neurosci Res 2007;85:1194-204.

Bryleva EY, Rogers MA, Chang CC, Buen F, Harris BT, Rousselet E, Seidah NG, Oddo S, LaFerla FM, Spencer TA, Hickey WF, Chang TY. ACAT1 gene ablation increases 24(S)-hydroxycholesterol content in the brain and ameliorates amyloid pathology in mice with AD. Proc Natl Acad Sci U S A 2010;107(7):3081-6.

Buxbaum JD, Cullen EI, Friedhoff LT. Pharmacological concentrations of the HMG-CoA reductase inhibitor lovastatin decrease the formation of the Alzheimer beta-amyloid peptide in vitro and in patients. Front Biosci 2002;7:50-9.

Cordy JM, Hussain I, Dingwall C, Hooper NM, Turner AJ. Exclusively targeting beta-secretase to lipid rafts by GPI-anchor addition up-regulates beta-site processing of the amyloid precursor protein. Proc Natl Acad Sci USA 2003;100:11735–40.

Deng JY, Huang JP, Lu LS, Hung LM. Impairment of cardiac insulin signaling and myocardial contractile performance in high-cholesterol/fructose-fed rats. Am J Physiol Heart Circ Physiol 2007;293(2):H978-87.

Dietschy JM, Turley SD. Thematic review series: brain lipids. Cholesterol metabolism in the central nervous system during early development and in the mature animal. J Lipid Res 2004;45:1375-97.

Friedhoff LT, Cullen EI, Geoghagen NS, Buxbaum JD. Treatment with controlled-release lovastatin decreases serum concentrations of human beta-amyloid (A beta) peptide. Int J Neuropsychopharmacol 2001;4(2):127-30.

Ghribi O, Larsen B, Schrag M, Herman MM. High cholesterol content in neurons increases BACE, β-amyloid, and phosphorylated tau levels in rabbit hippocampus. Experimental Neurology 2006;200(2):460–67.

Goldstein JL, DeBose-Boyd RA, Brown MS. Protein sensors for membrane sterols. Cell 2006;124:35-46.

Granholm AC, Bimonte-Nelson HA, Moore AB, Nelson ME, Freeman LR, Sambamurti K. Effects of a saturated fat and high cholesterol diet on memory and hippocampal morphology in the middle-aged rat. J Alzheimers Dis 2008;14(2):133-45.

Guglielmotto M, Aragno M, Tamagno E, Vercellinatto, I, Visentin S, Medana C, Catalano MG., Smith MA., Perry G, Danni O, Boccuzzi G, Tabaton M. AGEs/RAGE

complex upregulates BACE1 via NF-kappaB pathway activation. Neurobiol Aging 2010. In Press. PMID:20638753.

Haass C. Take five-BACE and the gamma-secretase quartet conduct Alzheimer's amyloid beta-peptide generation. EMBO J 2004;23:483-88.

Ho L, Qin W, Pompl PN, Xiang Z, Wang J, Zhao Z, Peng Y, Cambareri G, Rocher A, Mobbs CV, Hof PR, Pasinetti GM. Diet-induced insulin resistance promotes amyloidosis in a transgenic mouse model of Alzheimer's disease. FASEB J 2004;18:902-4.

Hoyer S, Riederer P. Alzheimer disease--no target for statin treatment. A mini review. Neurochem Res 2007;32(4-5):695-706.

Ishii K, Tokuda T, Matsushima T, Miya F, Shoji S, Ikeda S, Tamaoka A. Pravastatin at 10 mg/day does not decrease plasma levels of either amyloid-beta (Abeta) 40 or Abeta 42 in humans. Neurosci Lett 2003;350(3):161-4.

Kirsch C, Eckert GP, Koudinov AR, Müller WE. Brain cholesterol, statins and Alzheimer's Disease. Pharmacopsychiatry 2003;36 Suppl 2:S113-9.

Kivipelto M, Solomon A. Cholesterol as a risk factor for Alzheimer’s disease—epidemiological evidence. Acta Neurologica Scandinavica 2006;114(185):50–57.

Koudinov AR, Koudinova NV. Cholesterol homeostasis failure as a unifying cause of synaptic degeneration. J Neurol Sci 2005; 230:233-40.

Lütjohann DA, Papassotiropoulos A, Bjorkhem I, Locatelli S, Bagli M, Oehring RD, Schlegel U, Jessen F, Rao ML, von Bergmann K, Heun R.. Plasma 24S-hydroxycholesterol (cerebrosterol) is increased in Alzheimer and vascular demented patients. J Lipid Res 2000;41:195-8.

Michikawa M. Cholesterol paradox: is high total or low HDL cholesterol level a risk for Alzheimer's disease? J Neurosci Res 2003;72:141-6.

Pappolla MA, Bryant-Thomas TK, Herbert D, et al. Mild hypercholesterolemia is an early risk factor for the development of Alzheimer amyloid pathology. Neurology 2003;61(2):199–205.

Parsons RB, Austen BM. Protein lipidation of BACE. Biochem Soc Trans 2005;33(Pt 5):1091-3.

Parsons RB, Subramaniam D, Austen BM. A specific inhibitor of cholesterol biosynthesis, BM15.766, reduces the expression of beta-secretase and the production of amyloid-beta in vitro. J Neurochem 2007;102(4):1276-91.

Prasanthi JR, Huls A, Thomasson S, Thompson A, Schommer E, Ghribi O. Differential effects of 24-hydroxycholesterol and 27-hydroxycholesterol on beta-amyloid precursor protein levels and processing in human neuroblastoma SH-SY5Y cells. Mol Neurodegener 2009;4:1.

Puglielli L, Konopka G, Pack-Chung E, Ingano LA, Berezovska O, Hyman BT, Chang TY, Tanzi RE, Kovacs DM. Acyl-coenzyme A: cholesterol acyltransferase modulates the generation of the amyloid beta-peptide. Nat. Cell Biol 2001;3: 905-12.

Puglielli L, Tanzi RE and Kovacs DM. Alzheimer’s disease: the cholesterol connection. Nature Neuroscience 2003;6:345-51.

Raffai RL, Weisgraber KH. Cholesterol: from heart attacks to Alzheimer's disease. J Lipid Res 2003;44(8):1423-30.

Refolo LM, Pappolla MA, Malester B, et al. Hypercholesterolemia accelerates the Alzheimer’s amyloid pathology in a transgenic mouse model. Neurobiology of Disease 2000;7(4):321-31.

Rushworth JV, Hooper NM. Lipid Rafts: Linking Alzheimer's Amyloid-β Production, Aggregation, and Toxicity at Neuronal Membranes. Int J Alzheimers Dis 2010;2011:603052.

Sambamurti K, Kinsey R, Maloney B, Ge Y-W and Lahiri DK. Gene structure and organization of the human β-secretase (BACE) promoter. FASEB J 2004;18:1034-6.

Serrano-Pozo A, Vega GL, Lütjohann D, Locascio JJ, Tennis MK, Deng A, Atri A, Hyman BT, Irizarry MC, Growdon JH. Effects of simvastatin on cholesterol metabolism and Alzheimer disease biomarkers. Alzheimer Dis Assoc Disord 2010;24(3):220-6.

Shobab LA, Hsiung GY, Feldman HH. Cholesterol in Alzheimer's disease. Lancet Neurol 2005;4(12):841-52.

Simons M, Keller P, Dichgans J, Schulz JB. Cholesterol and Alzheimer's disease: is there a link? Neurology 2001;57(6):1089-93.

Solomon A, Kivipelto M, Wolozin B, Zhou J, Whitmer RA. Midlife serum cholesterol and increased risk of Alzheimer's and vascular dementia three decades later. Dement Geriatr Cogn Disord 2009;28(1):75-80.

Tamagno E, Parola M, Bardini P, Piccini A, Borghi R, Guglielmotto M, Santoro G, Davit A, Danni O, Smith MA, Perry G, Tabaton M. Beta-site APP cleaving enzyme up-regulation induced by 4-hydroxynonenal is mediated by stress-activated protein kinases pathways. J. Neurochem 2005;92:628-36.

Thirumangalakudi L, Prakasam A, Zhang R, et al. High cholesterol-induced neuroinflammation and amyloid precursor protein processing correlate with loss of working memory in mice. Journal of Neurochemistry 2008;106(1):475-85.

Tong XK, Nicolakakis N, Fernandes P, Ongali B, Brouillette J, Quirion R, Hamel E. Simvastatin improves cerebrovascular function and counters soluble amyloid-beta, inflammation and oxidative stress in aged APP mice. Neurobiol Dis 2009;35(3):406-14.

Ullrich C, Pirchl M, Humpel C. Hypercholesterolemia in rats impairs the cholinergic system and leads to memory deficits. Mol Cell Neurosci 2010;45(4):408-17.

Vassar R. The beta-secretase, BACE: a prime drug target for Alzheimer's disease. J. Mol. Neurosci 2001;17: 157-70.

Wang Y, Muneton S, Sjövall J, Jovanovic JN, Griffiths WJ. The effect of 24S-hydroxycholesterol on cholesterol homeostasis in neurons: quantitative changes to the cortical neuron proteome. J Proteome Res 2008;7(4):1606-14.

Wolozin B. Cholesterol and the biology of Alzheimer's disease. Neuron 2004;41:7-10.

Xiong H, Callaghan D, Jones A, Walker DG, Lue LF, Beach TG, Sue LI, Woulfe J, Xu H, Stanimirovic DB, Zhang W. Cholesterol retention in Alzheimer's brain is responsible for high beta- and gamma-secretase activities and Abeta production. Neurobiol Dis 2008;29:422-37.

Zandi PP, Sparks DL, Khachaturian AS, Tschanz J, Norton M, Steinberg M, Welsh-Bohmer KA, Breitner JC; Cache County Study investigators. Do statins reduce risk of incident dementia and Alzheimer disease? The Cache County Study. Arch Gen Psychiatry 2005;62(2):217-24.

Zhang L, Bruce-Keller AJ, Dasuri K, Nguyen AT, Liu Y, Keller JN. Diet-induced metabolic disturbances as modulators of brain homeostasis. Biochim Biophys Acta 2009;1792:417-22.

Table legends.

Table 1. Plasma lipid profile of rats after 20 weeks of standard diet (CTRL) or high-fat diet (HF). Data are means ± SD. Statistical significance: *p<0.05; **p<0.01 vs. CTRL.

Table 2. 24-OH-cholesterol evaluated by LC-MS in plasma and brain of rats after 20 weeks of standard diet (CTRL) or high-fat diet (HF). Data are means ± SD. Statistical significance: *p<0.05; **p<0.01 vs. CTRL.

Figure legends.

Figure 1. Physiological parameters of rats after 20 weeks of standard diet (CTRL) or high-fat diet (HF) (Panel A). Oral glucose charge tolerance test performed on 12 hrs. fasting rats after 20 weeks of standard diet (CTRL) or high-fat diet (HF) (Panel B). Data are means ± SD of 5-7 rats per group. Statistical significance: *p<0.05; **p<0.01 vs CTRL .

Figure 2. Real time RT-PCR analysis for BACE1 and SREBP2 expression on total RNA extracted from brain of rats fed a standard diet (CTRL) or a high-fat diet (HF) (Panel A). Representative western blotting analysis of SREBP2 content in total extracts (total protein amount, panel B) or in nuclear extracts (active form, panel C), of HMG-CoA-R (Panel D) and of BACE1 content (panel E) in total extracts from brain of CTRL or HF rats. The histogram (F) reports the densitometric analysis of the brain protein levels of 5-7 rats per group. Data are means ± SD. Statistical significance: *p<0.05; **p<0.01 vs. CTRL.

Figure 3. Free cholesterol (Panel A) and 24-OH-cholesterol (Panel B) evaluated by LC-MS in total extracts from SK-N-BE cells treated with 20 μM cholesterol for up to 48 hrs. Data

are means ± SD of 3 different experiments. Statistical significance: *p<0.05; **p<0.01 vs. CTRL.

Figure 4. Real time RT-PCR analysis for BACE1 and SREBP2 expression on total RNA extracted from SK-N-BE cells treated with 20 μM cholesterol for up to 24 hrs (Panel A). Real time RT-PCR analysis for SREBP2 following chromatin immunoprecipitation assay for the evaluation of SREBP2 binding on the BACE1 promoter on DNA extracted from cholesterol-treated SK-N-BE cells (Panel B). Data are means ± SD of 3 different experiments. Statistical significance: *p<0.05; **p<0.01 vs. CTRL.

Figure 5. Representative western blotting analysis of SREBP2 content in nuclear extracts (active form, Panel A), of HMG-CoA-R (Panel C) and of BACE1 content (Panel E) in total extracts from SK-N-BE cells treated with 20 μM cholesterol for up to 48 hrs. The histograms (Panels B, D and F) reports the densitometric analysis of 3 different experiments. Data are means ± SD. Statistical significance: *p<0.05; **p<0.01 vs. CTRL.

Figure 6. Representative western blotting showing the effect of SREBP2 silencing on BACE1 expression on total protein extracts from SK-N-BE cells treated with 20 μM cholesterol. Cells were transfected with SREBP2-specific siRNA, then exposed to cholesterol. BACE1 protein content was compared to the non-silenced condition (Panel A). The histogram reports the densitometric analysis of 3 different experiments (Panel B). Data are means ± SD. Statistical significance: *p<0.05; **p<0.01 vs. CTRL.

A

	Body weight (grams)	Blood glucose (mg/dl)	Plasma insulin (mg/l)	HOMA index
CTRL	376 ± 51	83 ± 12	0.79 ± 0.18	0.13 ± 0.08
HF	493 ± 56*	92 ± 5	2.98 ± 1.18**	0.32 ± 0.05*

B

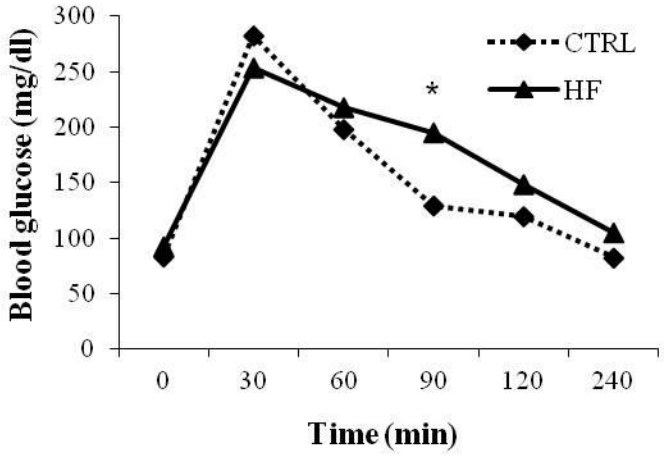

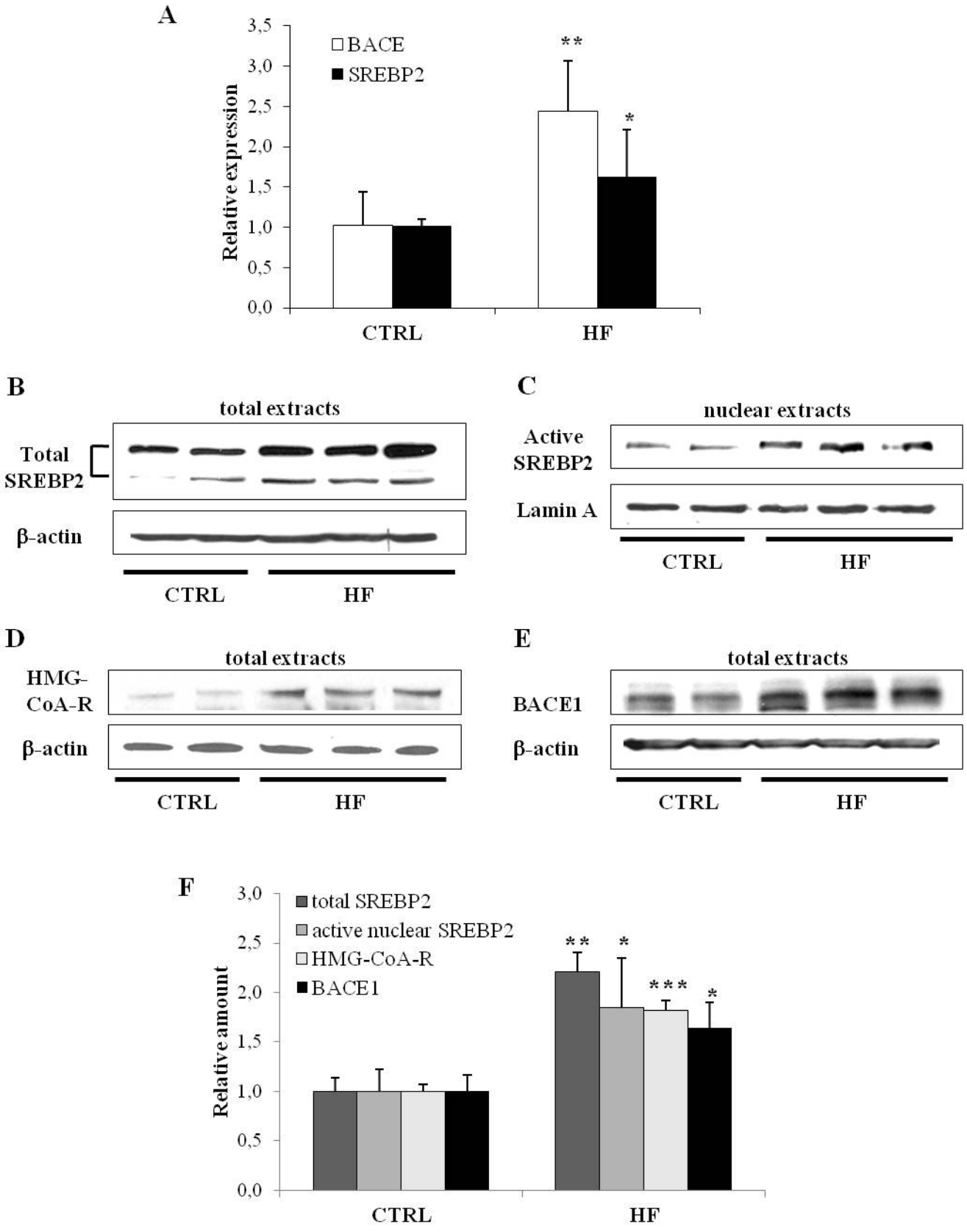
A
3,5
3,0
2,5
2,0
1,5
1,0
0,5
0,0
Relative expression
BACE
SREBP2
**
*
CTRL
HF
B
total extracts
Total SREBP2
β-actin
CTRL
HF
C
nuclear extracts
Active SREBP2
Lamin A
CTRL
HF
D
total extracts
HMG-CoA-R
β-actin
CTRL
HF
E
total extracts
BACE1
β-actin
CTRL
HF
F
3,0
2,5
2,0
1,5
1,0
0,5
0,0
Relative amount
total SREBP2
active nuclear SREBP2
HMG-CoA-R
BACE1
**
*
***
*
CTRL
HF

A

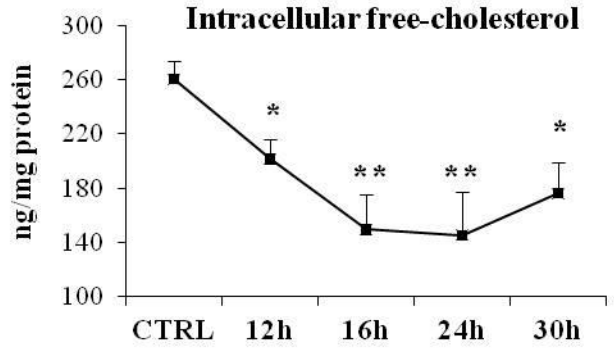
Intracellular free-cholesterol
ng/mg protein
300
260
220
180
140
100
*
**
**
*
CTRL
12h
16h
24h
30h

B

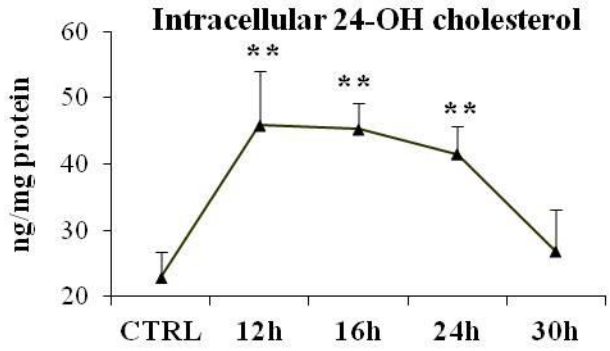
Intracellular 24-OH cholesterol
ng/mg protein
60
50
40
30
20
**
**
**
CTRL
12h
16h
24h
30h

A

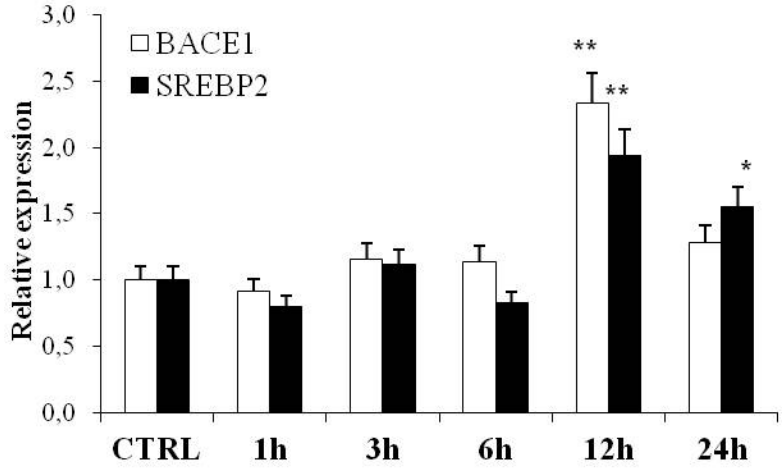
3,0
2,5
2,0
1,5
1,0
0,5
0,0
Relative expression
BACE1
SREBP2
**
**
*
CTRL
1h
3h
6h
12h
24h

B

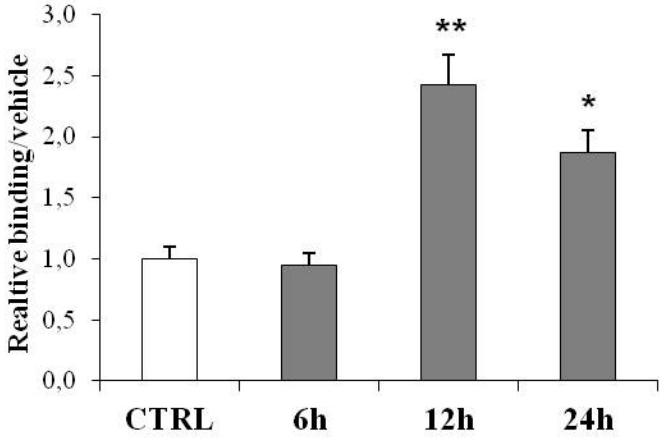
3,0
2,5
2,0
1,5
1,0
0,5
0,0
Realtive binding/vehicle
**
*
CTRL
6h
12h
24h

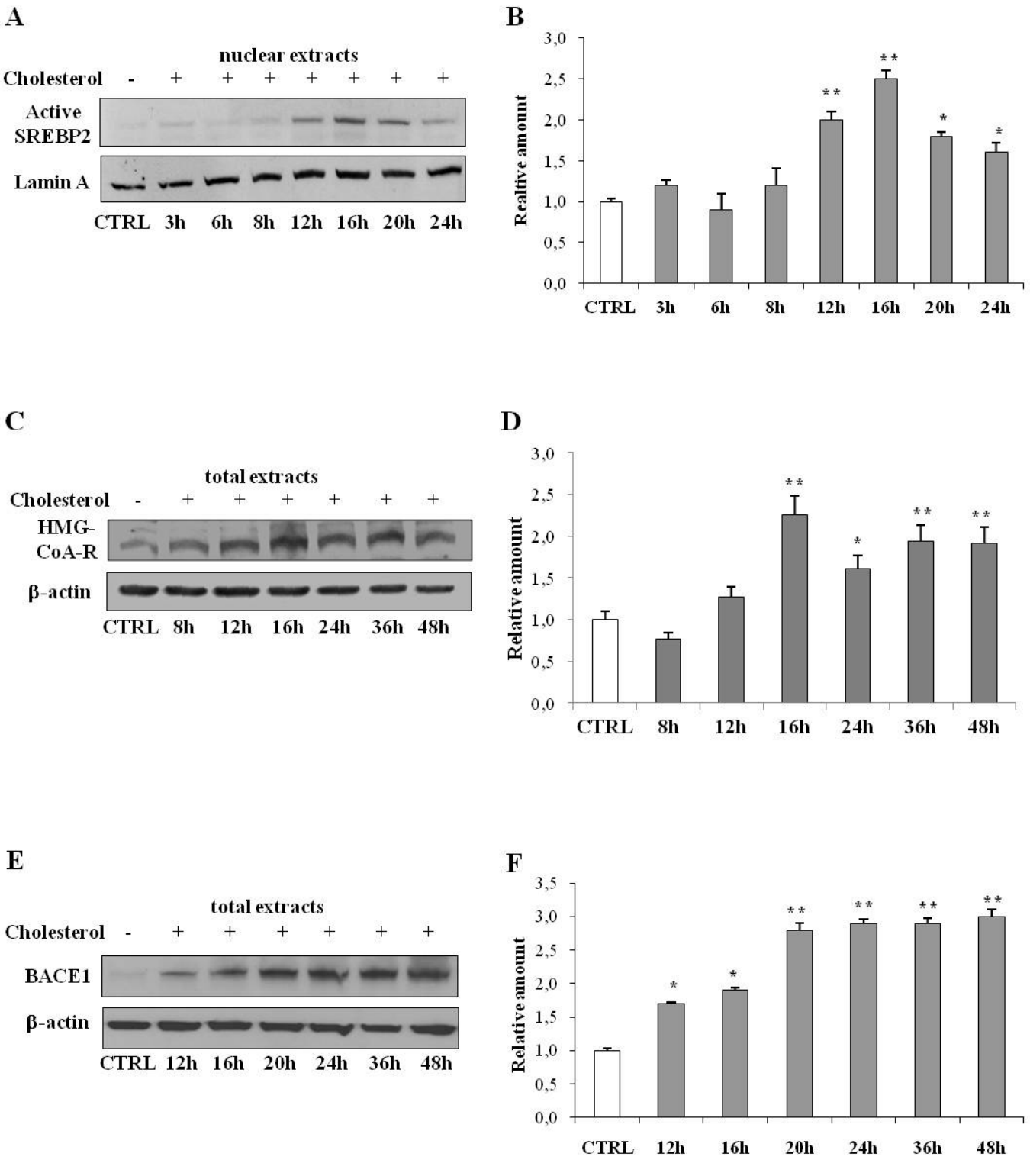
A
nuclear extracts
Cholesterol - + + + + + + +
Active SREBP2
Lamin A
CTRL 3h 6h 8h 12h 16h 20h 24h
B
Realtive amount
3,0
2,5
2,0
1,5
1,0
0,5
0,0
CTRL 3h 6h 8h 12h 16h 20h 24h
C
total extracts
Cholesterol - + + + + + + +
HMG-CoA-R
β-actin
CTRL 8h 12h 16h 24h 36h 48h
D
Relative amount
3,0
2,5
2,0
1,5
1,0
0,5
0,0
CTRL 8h 12h 16h 24h 36h 48h
E
total extracts
Cholesterol - + + + + + + +
BACE1
β-actin
CTRL 12h 16h 20h 24h 36h 48h
F
Relative amount
3,5
3,0
2,5
2,0
1,5
1,0
0,5
0,0
CTRL 12h 16h 20h 24h 36h 48h

A

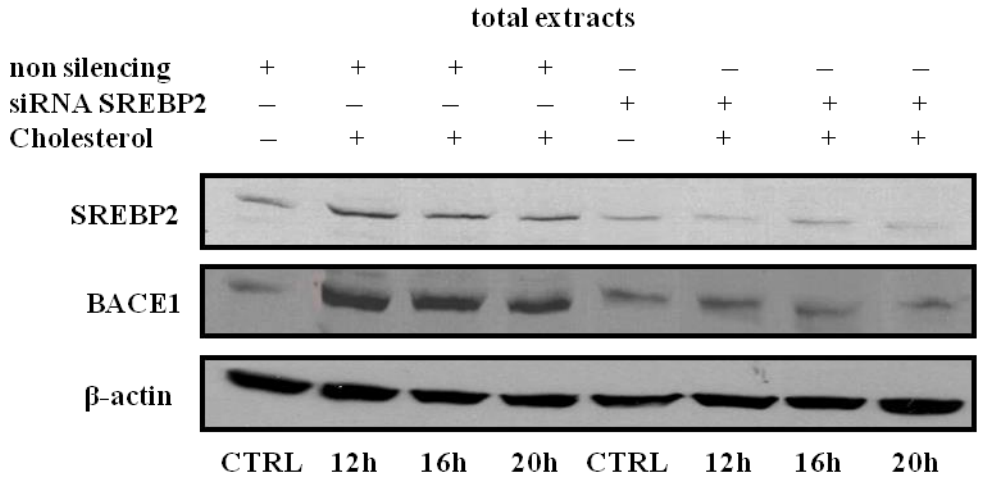
total extracts
non silencing + + + + – – – –
siRNA SREBP2 – – – – + + + +
Cholesterol – + + + – + + +
SREBP2
BACE1
β-actin
CTRL 12h 16h 20h CTRL 12h 16h 20h

B

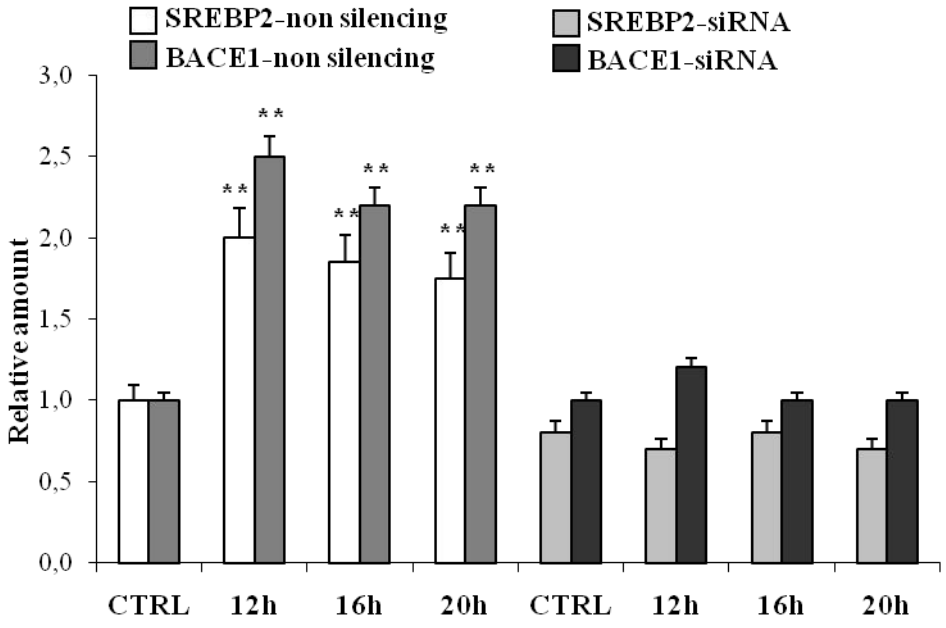
SREBP2-non silencing
BACE1-non silencing
SREBP2-siRNA
BACE1-siRNA
Relative amount
3,0
2,5
2,0
1,5
1,0
0,5
0,0
CTRL 12h 16h 20h CTRL 12h 16h 20h